Chemokine signaling in innate immunity of zebrafish embryos

Cui, C.

Chapter 4

Knockout analysis of zebrafish CXC chemokine receptor Cxcr3.2 demonstrates a function in macrophage migration to bacterial infection sites

Chao Cui, Vincenzo Torraca, Ralf Boland, Jan-Paul Bebelman, Marco Siderius, Martine Smit, Michiel van der Vaart, Catherine A. Loynes, Steven A. Renshaw, Astrid M. van der Sar, Herman P. Spaink, and Annemarie H. Meijer

Abstract

Despite increasing use of the zebrafish embryo for studying host-pathogen interactions, the chemokines and receptors involved in migratory responses of leukocytes during infection remain unknown. We have previously shown that *cxc chemokine receptor 3.2* (*cxcr3*.2), a homolog of human *CXCR3,* is expressed specifically in macrophages of one-day old zebrafish embryos. Using a GFP reporter construct and deep sequencing data of embryonic leukocyte populations, we demonstrate that during larval development *cxcr3.2* continues to be expressed in macrophages, with an over two fold higher expression level than in neutrophils. To investigate the function of *cxcr3.2* in macrophage behavior we employed a knockout mutant zebrafish line. When zebrafish embryos were infected by intravenous injection of *Salmonella typhimurium* or *Mycobacterium marinum*, there was no significant impact of *cxcr3.2* deficiency on the outcome of infection. In contrast, when these bacterial pathogens were locally injected into the hindbrain ventricle, we found that *cxcr3.2* knockout partially impaired the recruitment of macrophages to the infection site. Furthermore, *cxcr3.2* knockout embryos showed a reduced ability to control local hindbrain infections with attenuated *S. typhimurium* and *M. marinum* strains. Hindbrain injection of purified Cxcl11 protein, an infection-inducible chemokine in zebrafish, resulted in chemoattraction of macrophages in wild type but not in *cxcr3.2* mutant embryos. Based on these results, we propose that ligand-receptor interaction of Cxcl11 and Cxcr3.2 is important for macrophage migration in response to bacterial infection.

Introduction

Chemokines are small chemotactic cytokines that can direct migration and activation of leukocyte subpopulations as well as non-hematopoietic cells. These actions are mediated by chemokine receptors, which are a family of 7-transmembrane G protein-coupled receptors that are expressed on the surface of different cell types. Chemokines are classified into four subgroups (CXC, CC, C, and CX3C) dependent on the presence and position of conserved cysteine residues. Based on their functional properties, they are also grouped into homeostatic chemokines and inflammatory chemokines (Moser and Willimann, 2004). Homeostatic chemokines are constitutively produced and control leukocyte traffic during hematopoiesis, in the secondary lymphoid organs, and in immune surveillance of healthy peripheral tissues. They also control processes not related to the immune system. Inflammatory chemokines control the recruitment of leukocytes towards sites of infection, inflammation, and tissue injury, and towards tumours. The CXC subgroup chemokines orchestrate trafficking of cells of both the innate and adaptive immune system. Their receptors, belonging to the CXCR

family, are well conserved between human and other vertebrates, including fish, the earliest group of animals with innate and adaptive immunity.

The human chemokine receptor CXCR3 and its ligands, CXCL9, CXCL10, and CXCL11, are known to play important roles in several inflammatory and auto-immune diseases (Müller *et al*., 2010; Lacotte *et al*., 2009; Liu *et al*., 2005). CXCR3 has also been implicated in several malignancies and may serve as a biomarker of tumor behavior and potential therapeutic target (Fulton *et al*., 2009). Many studies have focused on the function of CXCR3 in T cells. CXCR3 is induced on naïve T cells upon activation, and remains highly expressed on type-1 helper (Th1)-type $CD4^+$ T cells and effector $CD8^+$ T cells (Liu *et al*., 2005). CXCR3 ligands promote Th1 cell maturation and regulate the generation and subsequent migration of effector T-cells into inflamed peripheral tissue (Groom *et al*., 2011). CXCR3 is also expressed on natural killer (NK) cells, neutrophils, macrophages, and endothelial cells. Recently, CXCR3 in mouse was shown to play an important role in macrophage-mediated vascular remodeling in response to hemodynamic forces (Zhou *et al*., 2010). In this study the perivascular accumulation of macrophages was shown to depend on CXCR3 signaling, and CXCR3 was found to contribute to selective features of macrophage activation required for extracellular matrix turnover and vascular remodeling. CXCR3 signaling was also suggested to be involved in the development of thymic metallophilic macrophages (Milićević *et al*., 2011). Furthermore, CXCR3 signaling was found to play a critical role in the murine neonatal response to sepsis (Cuenca *et al*., 2011). In neonates, which rely heavily on their innate immune system, CXCR3 expression on peritoneal macrophages and granulocytes increased following sepsis. Blockade of the ligand CXCL10 decreased the recruitment of peritoneal granulocytes and macrophages, and mortality was increased both by CXCL10 blockade or CXCR3 knockout.

Zebrafish is increasingly used as a model organism for studying chemokine signaling, since the transparency of embryos dramatically facilitates the visualization of cell migration processes (Raz and Mahabaleshwar, 2009). More than 100 chemokines and 40 chemokine receptor genes have been identified in the zebrafish genome (Nomiyama *et al*., 2008). The CXCR receptor family is well conserved between human and zebrafish, while some of its members, including CXCR3, CXCR4 and CXCR7, have been duplicated in zebrafish. Many studies in zebrafish have focused on the Cxcr4b/Cxcr7b-Cxcl12a axis, which plays critical roles in axon guidance, germ cell migration, and neuromast primordium migration (Miyasaka *et al*., 2007; Dumstrei *et al*., 2004; Knaut and Schier, 2008; Boldajipour *et al*., 2008; Mahabaleshwar *et al*., 2008; Haas and Gilmour, 2006; Dambly-Chaudière *et al*., 2007 ; Valentin *et al*., 2007). A role for Cxcr4b in tolerance to lipopolysaccharide-induced inflammation has also been proposed (Novoa *et al*., 2009). Cxcr1 and Cxcr2, the receptors for pro-inflammatory Cxcl8 (interleukin-8) signaling, were shown to be expressed in zebrafish leukocytes and intestinal

epithelial cells (Oehlers *et al*., 2010). However, the functions of chemokine receptors underlying leukocyte migration during bacterial infection and inflammation in zebrafish embryos remain unknown.

Using microarray analysis, we have previously identified an early leukocyte-specific chemokine receptor gene, *cxc chemokine receptor 3.2* (*cxcr3.2*), which is the possible counterpart of human *CXCR3*. Unlike the second *CXCR3* homolog, *cxcr3.1*, which is located on the same chromosome, *cxcr3.2* was shown to be expressed specifically in macrophages of one-day-old zebrafish embryos and to be dependent on the presence of the hematopoietic transcription factor Pu.1/Spi1 (Zakrzewska *et al.*, 2010; Chapter 2). Furthermore, antisense morpholino knockdown studies suggested that *cxcr3.2* is involved in the migration of macrophages to local sites of bacterial infection in the zebrafish embryo (Zakrzewska *et al.*, 2010; Chapter 2).

In this study, we employed a *cxcr3.2* mutant zebrafish line to investigate the function of *cxcr3*.2 in the behavior of embryonic leukocytes. To this end we used two well characterized zebrafish infection models, based on micro-injection of *Salmonella typhimurium* and *Mycobacterium marinum* bacteria (van der Sar *et al*., 2003, Davis *et al.*, 2002). In agreement with our previous morpholino knockdown results, we show that *cxcr3.2* knockout partially impairs bacterial-induced macrophage migration, which leads to insufficient macrophage recruitment to infection foci and decreased bacteria clearance. Based on injection of purified zebrafish chemokine Cxcl11 protein in wild type and cxcr3.2 mutant embryos, we could identify this chemokine as a putative ligand of Cxcr3.2 and propose that Cxcl11-Cxcr3.2 interaction is important for macrophage migration in inflammatory responses.

Materials and methods

Zebrafish husbandry

Zebrafish were handled in compliance with the local animal welfare regulations and were raised and maintained under standard laboratory conditions (http://ZFIN.org). Embryos were raised at 28.5°C in egg water (60 µg/ml Instant Ocean sea salts). Pigmentation was inhibited using 1-phenyl-2-thiourea (PTU; Sigma). For the duration of bacterial injections embryos were kept under anesthesia in egg water containing 0.02% buffered 3-aminobenzoicacidethylester (tricaine; Sigma).

cxcr3.2 *mutant and genotyping*

The *cxcr3.2*^{hu6044} mutant line, which carries a *cxcr3.2*^{T195G} stop mutation, was obtained from the Hubrecht Laboratory and the Sanger Institute Zefrafish Mutation

Resource. Heterozygous carriers of the mutation were outcrossed twice against wild type (AB/TL strain), and were subsequently incrossed. Genotyping zebrafish embryos and adults were done by restriction analysis after PCR. Genomic DNA was amplified using forward primer 5'-TACTTTAAGATGCTGAAATGACCAAGATA TTGAAAGGCATCTTTTTTGTTACAGCCTACAGCTTA -3' and reverse primer 5'-AGGAAACAGCTATGACCATAGCCAGGTATCTGTCAAAGC -3' and the product of this reaction was digested with DdeI (New England Biolabs). Fragments were analyzed on 2% agarose (Difco) gel. The PCR product of the wild type allele is cut by DdeI into two fragments of ca. 300 and 200 bp. PCR amplication introduces an extra DdeI site at the *cxcr3.2* mutation locus, which cuts the 300 bp fragment into fragments of ca. 250 and 50 bp.

cxcr3.2 *reporter construct*

A bacterial artificial chromosome (BAC) (DKEY-81P7) containing the *cxcr3.2* gene and promoter sequences was modified by the use of a red recombinase system in EL250 cells (Lee *et al*., 2001). The yeast transcription factor GAL4 was inserted at the *cxcr3.2* translation start site. A Medaka tol2 transposon cassette, named iTol2, was introduced in the BAC to increase efficiency of recombination (Suster *et al*., 2011). To determine expression overlap with macrophages the *cxcr3.2:GAL4* BAC construct was co-injected with a *UAS-E1b:nfsB.mCherry* construct (Davison *et al*., 2007) into embryos of Tg(*mpeg1:egfp*)^{gl22} transgenic zebrafish (Ellett *et al*., 2011). To determine expression overlap with neutrophils the *cxcr3.2:GAL4* BAC construct was injected into double transgenic zebrafish of the Tg(*UAS-E1b:nfsB.mCherry*)^{i149} (Davison *et al*., 2007) and Tg(*mpx:egfp*)^{i114} (Renshaw *et al*., 2006) lines.

cxcr3.2 *expression analysis in RNA-seq data sets*

GFP-positive and GFP-negative cell fractions were obtained by fluorescence-activated cell sorting (FACS) from 5 days post fertilization (dpf) larvae of Tg(*mpeg1:egfp*)^{gl22} (Ellett *et al*., 2011), Tg(*mpx:gfp*)^{i114} (Renshaw *et al*., 2006), and Tg(*lck:gfp*)^{cz1} (Langenau *et al*., 2004) transgenic lines as described in Cui *et al.*, 2011 (Chapter 1). RNA-seq libraries were prepared for Illumina sequencing as described by Kanwal (2012)**.**

Mpx activity staining and L-plastin immunofluorescence

Combined Mpx activity staining and immunofluorescence detection of L-plastin was performed essentially as described (Cui *et al*., 2011; Chapter 1). Briefly, embryos were fixed in 4% paraformaldehyde and Mpx activity staining was performed using the Peroxidase (Myeloperoxidase) Leukocyte Kit (Sigma-Aldrich). Stained embryos were then dehydrated for detection of L-plastin immunofluorescence using a rabbit

anti L-plastin primary antibody (Mathias *et al*., 2006) and goat anti-rabbit Alexa Fluor 488-conjugated secondary antibody (Invitrogen).

Bacterial strains and growth conditions

Infection experiments were performed with *Salmonella enterica* serovar Typhimurium *(S. typhimurium)* LPS mutant strain (Ra) SF1592 (van der Sar *et al*., 2003) and with the following *Mycobacterium marinum* strains: Mma20 (van der Sar *et al.*, 2004), MmM (Volkman *et al*., 2004), E11 (van der Sar *et al.*, 2004), ΔRD1 mutant (Volkman *et al*., 2004), FAM53 mutant (Stoop *et al.*, 2011). *S. typhimurium* were freshly grown overnight on LB agar plates supplemented with 100 µg/ml carbenicillin, and resuspended in phosphate-buffered saline (PBS) prior to injection of zebrafish embryos. *M. marinum* were grown overnight at 28.5 °C in Difco Middlebrook 7H9 broth (BD Biosciences) supplemented with 10% albumin-dextrose-catalase (BD Biosciences) and 0.05% Tween 80 (Sigma-Aldrich), and the appropriate antibiotics. Harvested bacteria were resuspended to the desired concentration in 2% polyvinylpyrrolidone (PVP40) in PBS (w/v) for injection of zebrafish embryos.

Bacterial infection studies

Embryos were staged at 28 hours post fertilization (hpf) by morphological criteria (Kimmel *et al*., 1995) and infected with either DsRed-expressing *S. typhimurium* Ra bacteria or with mCherry-expressing *M. marinum* strains. Bacteria were injected into the blood island for systemic infection, or injected into the hindbrain ventricle for local infection. As a control an equal volume of PBS was likewise injected. Injections were controlled using a Leica M50 stereomicroscope together with a FemtoJet microinjector (Eppendorf) and a micromanipulator with pulled microcapillary pipettes. Infected embryos were kept in egg water at 28 °C prior to live imaging or fixation. Pools of 20-40 embryos were collected for image analysis at stages as indicated in the figure legends.

Stereo fluorescence imaging of infections and pixel quantification

Anesthetized infected embryos were mounted in 1.5% methyl cellulose and aligned in the correct position on a 1% agarose layered Petri dish covered with egg water for imaging under a Leica MZ16FA fluorescence stereo microscope with Leica DFC420C camera. Fluorescent signal of bacteria in the images were analyzed using pixel quantification software as described (Stoop *et al*., 2011).

Confocal imaging analysis

Zebrafish embryos and larvae were mounted with low melting point agarose for confocal imaging. Confocal z-stacks were collected using a Leica TCS SPE

confocal microscope with HC PL APO CS 20x objective lens (N.A. 0.7), and processed and analyzed using IMARIS 7.4.0 (Bitplane AG). The confocal z-stacks were reconstructed into 3D image projections. Pixels showing fluorescence intensities above selected threshold levels in both channels were defined as showing colocalization. The numbers of these pixels was counted using Imaris software.

Cxcl11 *chemokine injections*

Cxcl11 protein purification and hindbrain injections were performed as described in Chapter 3.

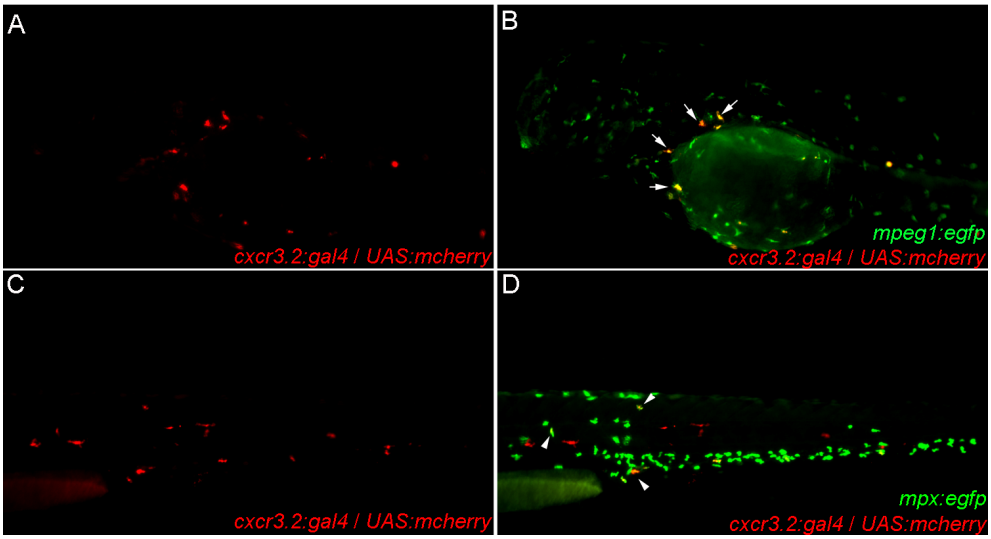

Figure 1. Transient expression of a *cxcr3.2* promoter-driven fluorescent reporter in transgenic zebrafish embryos. *cxcr3.2:gal4* and *UAS:mCherry* constructs were analyzed in *mpeg1:egfp* (A, B) and *mpx:egfp* (C, D) transgenic backgrounds. (A, B) Overlap of *cxcr3.2* reporter expression with macrophages. Images show mCherry signal (A) and the overlap between mCherry and egfp signals in the head and trunk region of a 2 dpf embryo (B). Transient expression of *cxcr3.2* promoter-driven mCherry showed considerable overlap with expression of the macrophage-specific marker *mpeg1:egfp* (arrows). (C, D) Partial overlap of *cxcr3.2* reporter expression with neutrophils. Images show mCherry signal (C) and the overlap between mCherry and egfp signals in the head and trunk region of a 2 dpf embryo (D). Expression of the *cxcr3.2* reporter marked a distinct leukocyte population from *mpx:egfp* marked neutrophils, while some overlap with *mpx:egfp* expressing cells was also observed (arrow heads).

Results

Expression levels of cxcr3.2 *in different leukocyte populations of zebrafish embryos and larvae.*

Previously we have shown by fluorescent *in situ* hybridization that the expression of chemokine receptor *cxcr3.2* overlaps specifically with that of *csf1r*-expressing macrophages of 1-day-old zebrafish embryos, while no overlap was detected at this stage of development with cells expressing the neutrophil marker *mpx* (Chapter 2). However, we were unable to detect *cxcr3.2* expression by *in situ* hybridization at later stages of development. To further investigate the *cxcr3.2* expression pattern we therefore used a fluorescent reporter driven by the *cxcr3.2* promoter. Transient expression of *cxcr3.2* promoter-driven mCherry expression showed considerable overlap with expression of the macrophage-specific *mpeg1:egfp* marker (Fig. 1).

Table 1. *cxcr3.2* expression levels in RNA-seq data of FACS-sorted macrophages, neutrophils, and immature T-cells[1]

Gene	*mpeg1:egfp* $^{+}$				*mpx:egfp* $^{+}$			*lck:egfp* $^{+}$		*egfp* $^{-}$
	#1	#2	#3	#4	#1	#2	#3	#1	#2	avg
cxcr3.2	35	74	112	28	29	3	46	0	0	3
cxcr3.1	3	3	4	0	0	0	0	8	6	1
mpeg1	24	223	157	98	0	4	31	0	0	5
mpx	4	19	125	0	872	192	922	0	0	2
lck	0	1	3	0	0	0	0	246	228	3

[1] RNA-seq libraries were constructed by Illumina sequencing of RNA from EGFP-positive (+) and negative (-) cell fractions obtained by dissociating and FACS-sorting 5-6 dpf larvae of *mpeg1:egfp*, *mpx:egfp*, and *lck:egfp* transgenic zebrafish (Kanwal, 2012). RPKM values are shown for 2-4 biological replicates of EGFP-positive cells per line. The RPKM value for EGFP-negative cells is the average of all libraries. RPKM values of chemokine receptor genes *cxcr3*.2 and *cxcr3*.1 are shown in comparison to those of *mpeg1*, *mpx*, and *lck*, as markers for macrophages, neutrophils, and immature T-cells, respectively.

In addition, it marked a population of leukocytes distinct from those marked by *mpx:egfp*, while also some overlap with *mpx:egfp* expressing cells was observed (Fig. 1). These results require further confirmation with a stable transgenic line, but support that *cxcr3.2* is expressed predominantly in macrophages, and in a subset of neutrophils of zebrafish larvae. We also investigated *cxcr3.2* expression by RNA sequencing (RNA-seq) analysis of macrophage, neutrophil, and immature T-cell populations obtained by fluorescence-activated cell sorting (FACS) of *mpeg1:egfp*, *mpx:egfp*, and *lck:egfp* transgenic larvae at 5-6 dpf. Comparison of the expression

levels in these cells by RPKM values (read counts per kilobase of transcript per million mapped reads) showed that highest expression levels of *cxcr3*.2 correlated with *mpeg1:egfp*-positive cells and were on average ca. 2.5-fold higher in *mpeg1:egfp*-positive cells compared with *mpx:egfp*-positive cells (Table 1). Expression of *cxcr3.1*, the second *CXCR3* homolog in zebrafish, was more than 20-fold lower in *mpeg1:egfp*-positive cells compared with *cxcr3.2* expression, and was not detectable in *mpx:egfp*-positive cells. In contrast, *cxcr3.*1 expression was detectable in *lck:egfp*-positive cells, while expression of *cxcr3.2* was not. Taken together, we conclude that *cxcr3.2* is predominantly expressed in zebrafish embryonic macrophages, but at later stages of development is also expressed in neutrophils.

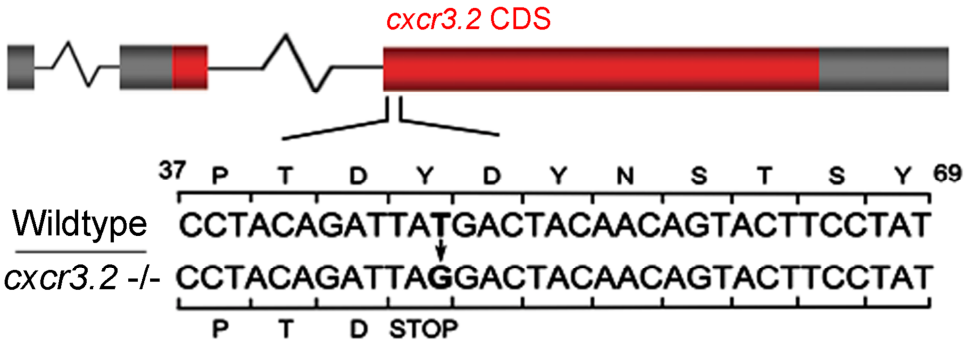

Figure 2. Schematic overview of the point mutation in the *cxcr3.2-/-* line. The DNA and amino acid sequence of wild type and mutant are shown around the T to G point mutation, which is located in the second coding exon of the *cxcr3.2* gene, at nucleotide position 48 with respect to the translation start site. The mutation results in a truncation of the protein at amino acid 16. Red bar, Coding DNA Sequence (CDS); grey bar, non-coding sequence.

Identification of a zebrafish knockout mutant in the leukocyte-specific chemokine receptor cxcr3.2

Resequencing of an N-ethyl-N-nitrosurea (ENU)-mutagenized zebrafish library resulted in the identification of a *cxcr3.2* mutant allele, *cxcr3.2*^{hu6044}, which carries a T to G point mutation creating an early stop codon (Fig. 2). The mutation leads to a truncation at amino acid 16, thus deleting almost the complete sequence of the 378 amino acid wild type Cxcr3.2 protein. Zebrafish embryos homozygous for the mutation (*cxcr3.2-/-*) were found at Mendelian frequencies after crossing of heterozygous parents and reached adulthood without showing differences in viability with their wild type siblings. Adult cxcr3.2-/- fish also showed normal fertility.

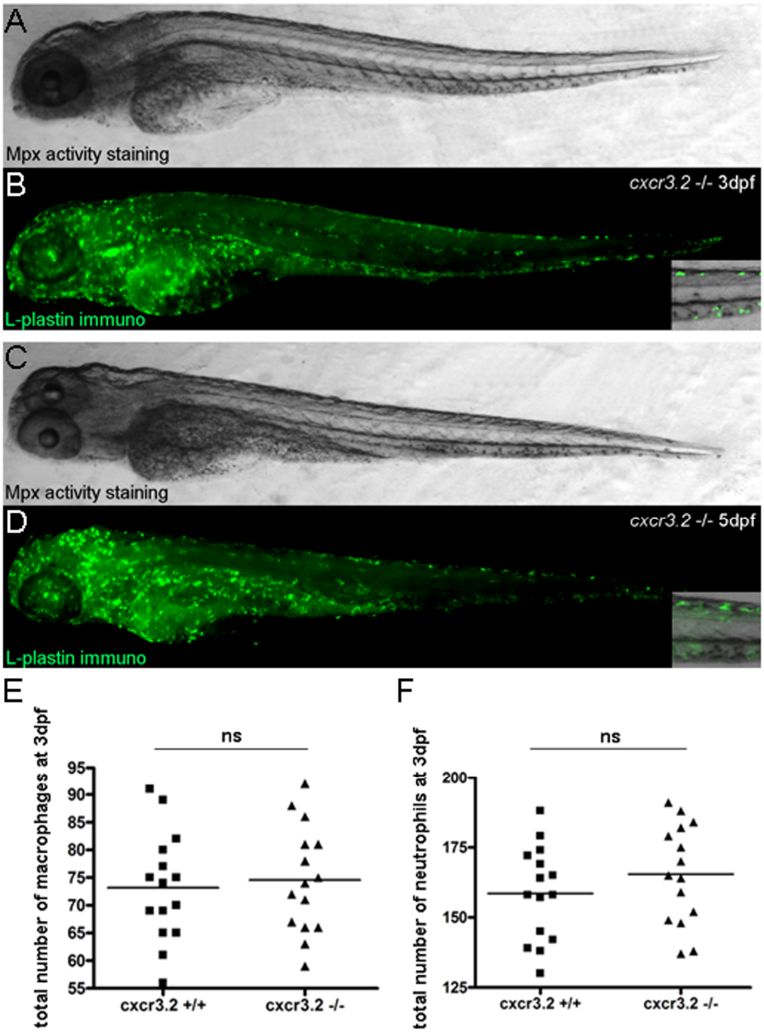

Figure 3. Normal development and leukocyte differentiation in *cxcr3.2* mutant embryos. (A-D) L-plastin immunofluorescence (B,D) and Mpx activity (A,C) staining of *cxcr3.2* mutant larvae at 3 (A,B) and 5 (C,D) dpf. Insets show details of L-plastin- and Mpx-positive cells in the caudal hematopoietic tissue. No overt differences were detected between wild types and mutants in larval morphology and localization patterns of macrophages (L-plastin$^+$, Mpx$^-$) and neutrophils (L-plastin$^+$, Mpx$^+$; note that neutrophil identity is determined based on Mpx$^+$ signal as the L-plastin fluorescence signal is not visible due to the black precipitate of the Mpx reaction). (E, F) Quantification of macrophages (E) and neutrophils (F) at 3 dpf by combined L-plastin immuno and Mpx activity staining. Each data point represents an individual embryo and lines indicate the mean value. Numbers of macrophages (L-plastin$^+$, Mpx$^-$) and neutrophils (L-plastin$^+$, Mpx$^+$) were similar in *cxcr3.2* mutant and wild type larvae (not significant (ns) by Student t-test).

Embryonic development and leukocyte differentiation in cxcr3.2 *mutant embryos*

Our previous morpholino knockdown studies have provided a preliminary description of the effect of Cxcr3.2 on leukocyte migration during infection in zebrafish embryos (Chapter 2). Cxcr3.2 morphants showed no detectable general developmental phenotype or difference in leukocyte differentiation by 2 dpf. At later stages no effective morpholino knockdown could be achieved. Using the *cxcr3.2* mutant zebrafish line, we further investigated the effects of *cxcr3.2* deficiency during embryonic and larval development (Fig. 3A-D). By 5 dpf, *cxcr3.2* mutant larvae did not display any overt morphological phenotype as compared to their wild type embryos. We then conducted a combination of myeloperoxidase (Mpx) activity assay and L-plastin immunofluorescence staining to visualize the entire population of leukocytes in *cxcr3.2* mutant and wild type embryos. The total number of Mpx-positive neutrophils and L-plastin-positive/Mpx-negative leukocytes (predominantly macrophages) were not altered in the *cxcr3.2* mutant larvae by 3 and 5 dpf (Fig. 3E, F), which indicates that *cxcr3.2* is not involved in early development and leukocyte differentiation.

Reduced macrophage migration to local S. typhimurium *and* M. marinum *infection sites in* cxcr3.2 *mutant embryos*

To confirm the function of Cxcr3.2 in bacteria-induced early macrophage migration as suggested by previous morpholino knockdown (Chapter 2), we performed hindbrain ventricle injection of zebrafish embryos at 28 hpf with red fluorescent *S. typhimurium* bacteria of a non-pathogenic LPS mutant strain (Ra) (Fig. 4A-D). Since neutrophils do not actively migrate into the hindbrain ventricle at this developmental stage, we analyzed the total number of L-plastin-positive cells that represent the macrophage population infiltrating the hindbrain. Consistent with the previous knockdown data, deficiency in *cxcr3.2* resulted in reduced macrophage migration ($P<0.001$) towards the *S. typhimurium* infection site at 3 hours post fertilization (hpi) (Fig. 4E), confirming that Cxcr3.2 contributes to bacteria-induced macrophage migration. Subsequently, we examined if Cxcr3.2 is also required for the attraction of macrophages to a local hindbrain infection with *M. marinum*. In *cxcr3.2* mutants the attraction of macrophages to *M. marinum* infection was slightly reduced compared to the number of macrophages accumulating in the hindbrain of wild type embryos ($P=0.056$). Notably, there was a significant difference between *S. typhimurium* and *M. marinum* hindbrain infections in the total numbers of attracted macrophages. Injection of *M. marinum* in the hindbrain of wild type embryos resulted in the accumulation of an average number of 8 macrophages at 3 hpi, which was approximately 1.5-fold lower than the average number of macrophages attracted to an infection with a similar dose of *S. typhimurium* Ra

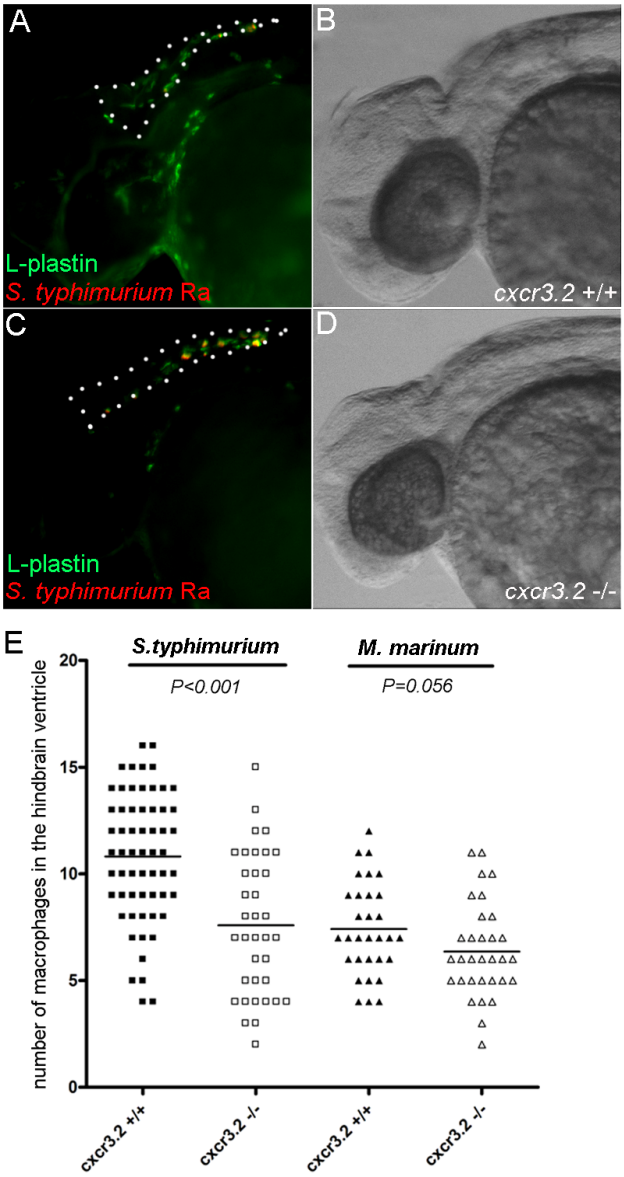

Figure 4. Macrophage migration towards local hindbrain infection with *S. typhimurium* Ra and *M. marinum* MmM in wildtype and *cxcr3.2* mutant embryos. (A-D) Representative images of hindbrain infection with 50 cfu of *S. typhimurium* in wild type (A, B) and *cxcr3.2* mutant embryos (C, D) at 3 hpi. Fluorescence images (A,C) show the signals of L-plastin-labeled macrophages and DsRed-labeled bacteria in the hindbrain, which is outlined with a dotted line; the corresponding bright field images (B,D) are included for reference. (E) Quantification of macrophage migration into the hindbrain in response to *S.*

typhimurium Ra and *M. marinum* MmM infection at 3 hpi. Each data point represents an individual embryo and lines indicate the mean value. *P* values indicate the level of statistical difference by Student t-test. *S. typhimurium*-induced macrophage migration was significantly reduced in *cxcr3.2* mutants, while a minor migration phenotype was detected with *M. marinum* infection (*P*=0.056).

bacteria in wild type embryos and similar to the average number of macrophages recruited to *S. typhimurium* Ra infection in *cxcr3.2* mutants. These data support the contribution of Cxcr3.2 to the early migration of macrophages to local infections with *S. typhimurium* and *M. marinum* infection. Furthermore, the higher recruitment of macrophages to *S. typhimurium* infection as compared to *M. marinum* infection appears to be largely mediated by Cxcr3.2-dependent signalling.

Cxcr3.2 function is required for restricting S. typhimurium *hindbrain infection*

To further evaluate the contribution of Cxcr3.2 to *S. typhimurium*-induced macrophage migration and development of hindbrain infection, we examined the number of macrophages and bacterial burden in the hindbrain at later stages. By 8 hpi, the number of macrophages in the hindbrain of mutant embryos reached a similar level as in wild type embryos, indicating that multiple factors contribute to the migration process, which partially compensate for the loss-of-function effect of *cxcr3.2* (Fig. 5A). In addition, wild type embryos and *cxcr3.2* mutants at 8 hpi showed no significant difference in bacterial burden as determined by fluorescent pixel quantification of DsRed-labelled *S. typhimurium* in stereo fluorescence microscopy images (Fig. 5B). Interestingly, we observed that the follow up migration of macrophages was not completely recovered in the *cxcr3.2* mutant embryos. By 24 hpi, the total number of *cxcr3.2*-/- macrophages in the hindbrain was significantly less than that in wild type embryos (Fig. 5A). In addition, the mean level of bacterial burden in *cxcr3.2* mutant embryos at 24 hpi was significantly higher (Fig. 5C). Furthermore, among 32 infected mutant embryos, 26 (78%) still showed remaining *S. typhimurium* Ra bacteria, while almost half of the wild type embryos had completely cleared the infection at 24 hpi. In contrast, no difference between wild type and *cxcr3.2* mutant embryos was observed upon intravenous infection with *S. typhimurium* Ra (Supplementary Figure S1). Thus, *cxcr3.2* deficiency affected bacterial clearance only in the hindbrain infection model, which requires attraction of macrophages to the infection site. In conclusion, our data demonstrate that Cxcr3.2 is essential for bacteria-induced early macrophage migration to localized infection, which has an important impact on bacterial clearance in zebrafish embryos.

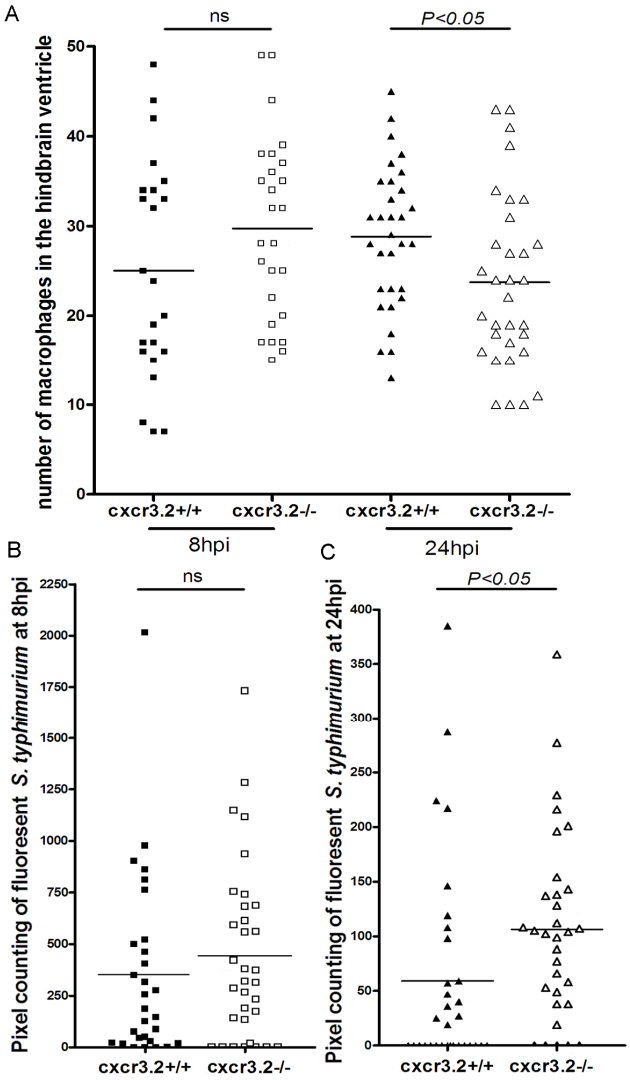

Figure 5. Progression of *S. typhimurium* Ra hindbrain infection in wild type and *cxcr3.2* mutant embryos. (A) Number of macrophages in the hindbrain of embryos infected with 50 cfu of *S. typhimurium* Ra strain at 8 and 24 hpi. Reduced macrophage migration towards *S. typhimurium* infection in *cxcr3.2* mutants at 3 hpi (Fig. 4) was recovered at 8 hpi. However, by 24 hpi, the total number of macrophages in the hindbrain was significantly less in *cxcr3.2* mutants as compared to the wild type. (B, C) Quantification of *S. typhimurium* Ra infection levels by fluorescent pixel counting in wild type and *cxcr3.2* mutant embryos at 8 hpi (B) and 24 hpi (C). Bacterial burden was significantly higher in *cxcr3.2* mutant embryos at 24 hpi. In all graphs, each data point represents an individual embryo and lines indicate the mean value. *P* values indicate the level of statistical difference by Student t-test (ns, not significant).

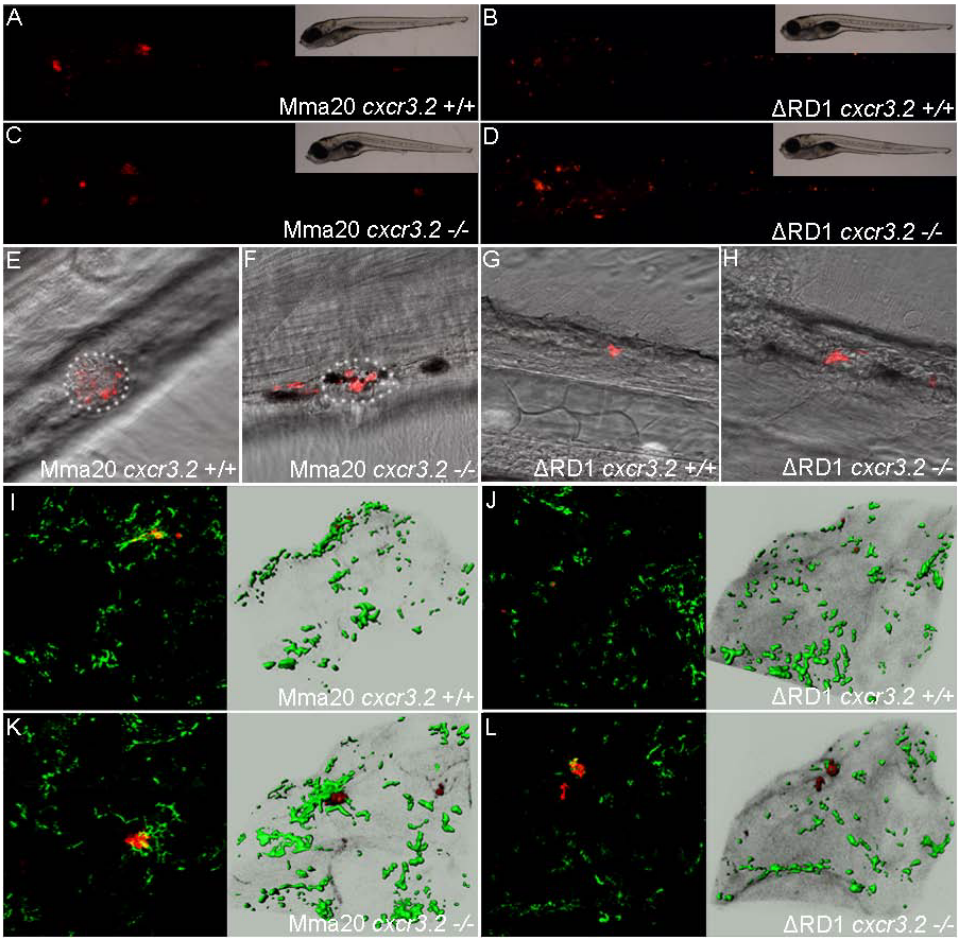

Figure 6. *M. marinum* infection in *cxcr3.2* mutants. (A-H) Systemic infection by injection of *M. marinum* strains into the blood island. Embryos were injected at 28 hpf with mCherry-labelled *M. marinum* of an Mma20 wild type strain (100 cfu, A, C, E, F) and an attenuated strain ΔRD1 strain (200 cfu, B, D, G, H). Representative stereo fluorescence images of infected embryos (A-D, with bright field images in insets) and confocal images of granuloma-like aggregates in these embryos (E-H) are shown. Quantification of bacterial burden by fluorescent pixel counting (Figure 7) showed no significant difference between the wild type and *cxcr3.2* mutant. Mma20 infection induced granuloma formation in tissues of both wild type embryos and *cxcr3.2* mutants (E, F, granuloma-like aggregates of infected and non-infected immune cells are outlined with a dotted line). ΔRD1 infection shows attenuated infection in wild type embryos and *cxcr3.2* mutants with no or poor granuloma formation; similar tissue migration of infected macrophages is observed in both cases (G, H). (I-L) Hindbrain ventricle infection with *M. marinum* strains. Wild type (I, J) and *cxcr3.2* mutant (K, L) embryos were injected at 28 hpf with 100 cfu of *M. marinum* Mma20 or 200 cfu of the ΔRD1 strain. Infected larvae were imaged at 5 dpi to show the mCherry-labelled *M. marinum* growth as well as the infiltration of L-plastin positive leukocytes in the hindbrain.

Representative confocal z-stacks (left images in I-L) and IMARIS 3D reconstructions (right images in I-L) of the infected hindbrain ventricles are shown with the *M. marinum* signal in red and the L-plastin signal in green. Quantification of bacterial burden and colocalization of *M. marinum* and L-plastin signal (Figure 7) revealed increased infection and more extracellular *M. marinum* bacteria in the *cxcr3.2* mutants (K, L) relative to wild type larvae (I, J).

cxcr3.2 *mutation does not prevent the induction of granuloma-like aggregates during* M. marinum *infection*

Zebrafish is a well characterized model for studying early stages of granuloma formation induced by mycobacterium infection, which represents a hallmark of tuberculosis (Ulrichs and Kaufmann, 2006; Ramakrishnan, 2012). The early granulomas in zebrafish larvae infected with *M. marinum* consist of tissue aggregates of infected macrophages and other leukocytes that are attracted to these infected cells. We analyzed the effect of *cxcr3.2* knockout on granuloma formation by performing intravenous infection at 28 hpf with *M. marinum.* At 5 days post infection (dpi) with *M. marinum* strain Mma20, *cxcr3.2* mutants and wild type embryos showed no significant differences in total bacterial burden as determined by fluorescent pixel quantification of mCherry-labelled bacteria in stereo fluorescence microscopy images (Fig. 6A-D, Fig. 7Ai). Upon infection with a less virulent strain, E11 (van der Sar *et al*., 2004), or with two attenuated mutant strains that are affected in granuloma formation (ΔRD1 (Davis and Ramakrishnan, 2009) and Fam53 (Stoop *et al.*, 2011)) *cxcr3.2* mutants seemed to carry slightly higher bacterial burdens, but differences with wild type embryos did not reach significance (Fig. 6C, D; Fig. 7Aii-iv). Notably, similar granuloma-like structures were also formed in tissues at different locations in the *cxcr3.2* mutant (Fig. 6E-H), which suggested that circulating macrophages in *cxcr3.2* mutant embryos are still capable of phagocytosing *M. marinum* bacteria injected in the circulation and are able to initiate tissue dissemination of the infection and granuloma formation.

Extracellular growth of M. marinum *strains in hindbrain-infected* cxcr3.2 *mutant embryos*

As the next step, we used the hindbrain injection site to further examine the *cxcr3.2* knockout effect on localized infections with different *M. marinum* strains. Wild type and *cxcr3.2* mutant embryos were injected with 100 cfu of the Mma20 and E11 strains, or with 200 cfu of the attenuated ΔRD1 and FAM53 strains, and fixed at 5 dpi for following L-plastin staining and determination of bacterial burden by fluorescence quantification. L-plastin-positive leukocytes (Alexa488-labeled) and mCherry-labeled bacteria in the hindbrain ventricle were imaged by confocal microscopy and IMARIS image analysis software was used for 3 dimensional

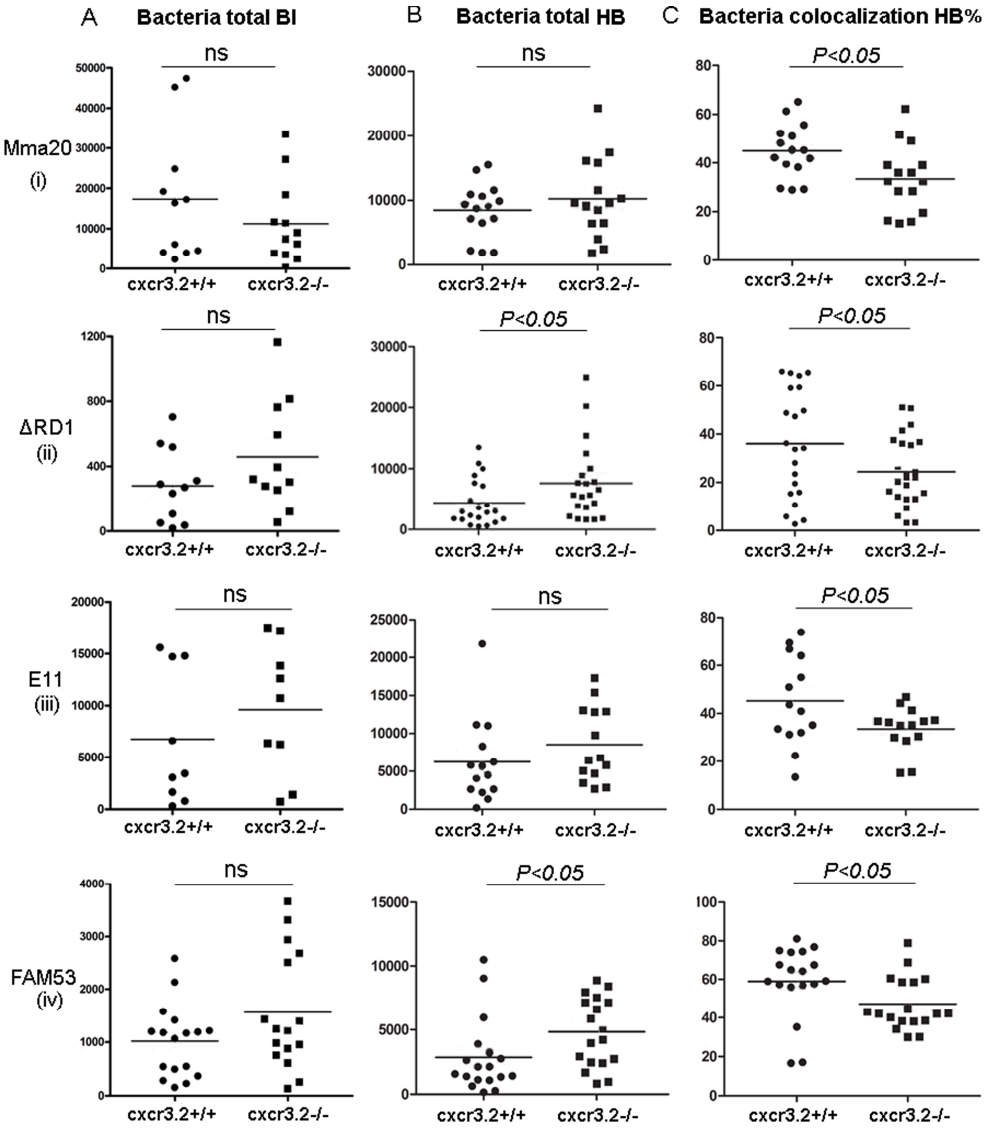

Figure 7. Quantification of infections with different *M. marinum* wild type and mutant strains in wild type and cx*cr3.2* mutant embryos. Infections were performed with mCherry-labelled *M. marinum* bacteria of the M-type strain Mma20 (i), a ΔRD1 mutant in M-strain background (ii), the E11 strain (iii), and a Fam*53* mutant in E11 background (iv). (A) Systemic infections by injection into the blood island (BI) at 28 hpf. Quantification of bacterial burden at 5 dpi was performed by fluorescent pixel quantification of stereo fluorescence images as shown in Figure 6A-D. No significant differences in bacterial growth were detected between wild type and *cxcr3.2* mutant embryos (Ai-Aiv). (B, C) Local infections by hindbrain ventricle (HB) injection at 28 hpf. Embryos were fixed at 5 dpi for L-plastin

immunostaining. IMARIS analysis of confocal z-stacks (representative images shown in Figure 6I-L) was performed to quantify the total bacterial fluorescence in the hindbrain (Bi-Biv) and the co-localization between red fluorescent *M. marinum* signal and green fluorescent L-plastin signal (Ci-Civ). ΔRD1 and Fam53 infections showed increased bacterial burden in *cxcr3.2* mutants (Bii, Biv), and all four *M. marinum* strains showed reduced co-localization with L-plastin-labelled cells in *cxcr3.2* mutants (Ci-Civ), indicating that more bacteria are extracellular in the mutant embryos. In all graphs, each data point represents an individual embryo and lines indicate the mean value with standard error. *P* values indicate the level of statistical difference by Student t-test (ns, not significant).

reconstruction of the infected areas from confocal z-stacks (Fig. 6I-L). In the 3D reconstructions, it was observed that *M. marinum* bacteria in the wild type embryos were mostly present inside L-plastin-labelled cell aggregates (Fig. 6 I, J). In contrast, more *M. marinum* bacteria appeared to remain extracellular in *cxcr3.2* mutant embryos (Fig. 6K, L). These observations were confirmed by IMARIS quantification of the total bacterial burdens (Fig. 7B) and the colocalization signals between L-plastin and mCherry-labeling (Fig. 7C). Bacterial burden was not significantly different between wild type and *cxcr3.2* mutant embryos in the infections with the Mma20 and E11 strains (Fig. 7 Bi and Biii), but infections with the attenuated ΔRD1 and FAM53 mutant strains resulted in an increased bacterial burden in the *cxcr3.2* mutant embryos by 5 dpi (Fig. 7Bii and Biv). Furthermore, infections with all four *M. marinum* strains consistently resulted in significantly reduced colocalization signals between L-plastin-labelled host immune cells and *M. marinum* bacteria in *cxcr3.2* mutants compared with wild type embryos (Fig. 7Ci-iv). From these differences in colocalization signals we conclude that higher percentages of *M. marinum* Mma20, E11, ΔRD1 and FAM53 bacteria are present intracellular in wild type embryos, while the strains show more extensive extracellular proliferation in *cxcr3.2* mutants. Therefore, we conclude that chemokine receptor Cxcr3.2 is essential for bacteria restriction within host immune cells during hindbrain infection of *M. marinum* in zebrafish embryos.

Purified zebrafish chemokine Cxcl11 induces Cxcr3.2-driven macrophage migration

The chemokine ligand for Cxcr3.2 is currently unknown. As described in chapter 3, we analyzed all known zebrafish CXC chemokines for similarity with the human chemokines CXCL9, 10 and 11, which are the ligands of CXCR3, the human homolog of zebrafish Cxcr3.2. We found that zebrafish Cxcl11 has a relatively close relationship to the human CXCR3 ligands and is also inducible upon *M. marinum* infection of zebrafish embryos. We selected the Cxcl11 chemokine for purification using a *Pichia pastoris* production system and showed a positive effect of the recombinant protein on attracting embryonic macrophages following hind-brain injection (Chapter 3). In order to check the interaction of this candidate ligand

with Cxcr3.2, we performed hindbrain injections with the purified protein in *cxcr3.2* mutant and wild type embryos at 28 hpf. Strikingly, by 2.5 hpi, the Cxcl11-driven macrophage migration that we observed in wild type embryos was significantly reduced in the *cxcr3.2* mutants (Fig. 8). Taken together, we could identify Cxcl11 as a putative ligand of Cxcr3.2 and propose that Cxcl11-Cxcr3.2 interaction is important for macrophage migration in the inflammatory response to bacterial infections in zebrafish embryos.

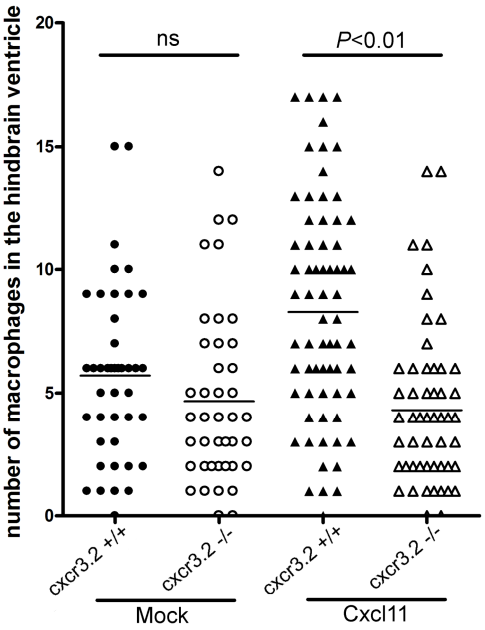

Figure 8. Cxcl11-induced macrophage migration is dependent on Cxcr3.2 signaling. Purified zebrafish chemokine Cxcl11 was injected into the hindbrain ventricle at 28 hpf. Injected embryos were fixed at 2.5 hpi followed by L-plastin immunofluorescence staining. Cxcl11 injection induced more macrophage migration in comparison with mock-injected control embryos (buffer alone), while this induction was significantly reduced in the *cxcr3.2* mutant embryos. Each data point represents an individual embryo and lines indicate the mean value. *P* values indicate the level of statistical difference by one-way ANOVA (ns, not significant).

Discussion

Host-pathogen interaction studies in zebrafish embryos require a better understanding of the chemokine signaling network underling immune cell migration in this model. The zebrafish contains homologs of the human CXC chemokine receptor family members, but their functions in inflammation and infection remain largely unknown. In this study, we have analyzed a knockout mutant of *cxcr3.2*, a homolog of human *CXCR3*, and show that this receptor gene is required for the migration of zebrafish embryonic macrophages towards local sites of *S. typhimurium* and *M. marinum* infection. Furthermore, we cells (Liu *et al.*, 2005; Zhou *et al.*, 2010; Cuenca *et al.*, 2011). *CXCR3* has two homologs in zebrafish, *cxcr3.1* and *cxcr3.2*. The presence of both genes in close vicinity on chromosome 16 suggests that these two genes result from a duplication event. RNA-seq profiles of macrophages (*mpeg1:egfp*-positive cells), neutrophils (*mpx:egfp*-positive), and T-lymphoblasts (*lck:egfp*-positive) from zebrafish larvae at 5 dpf showed that *cxcr3.1* and *cxcr3.2* have different expression patterns. Expression of *cxcr3.1* was etectable in *lck:egfp*-positive cells, while expression of *cxcr3.2* was not. Conversely, *cxcr3.2* expression was over 20-fold higher in myeloid cells than c*xcr3.1* expression. It is possible that after duplication of an ancestral *cxcr3* gene in zebrafish, functions in myeloid and lymphoid cells have been split over the two descendant genes. However, *cxcr3.1* and *cxcr3.2* expression levels in myeloid and lymphoid cells of adult zebrafish remain to be analyzed and might be more overlapping. RNA-seq-based expression of *cxcr3.2* in *mpeg1:egfp*-positive macrophages was more than two fold higher than in *mpx:egfp*-positive neutrophils. In agreement, previous *in situ* hybridization data of younger embryos (Chapter 2) and reporter gene expression driven by the *cxcr3.2* promoter showed predominant expression of *cxcr3.2* in macrophages. We therefore focused the present study on the function of *cxcr3.2* in macrophages.

We have previously demonstrated that knockdown of *cxcr3.2* using morpholinos partially reduces macrophage migration upon local bacterial challenge at 1 dpf (Chapter 2). However, it was not possible to achieve the knockdown effect longer than 2 dpf with the morpholino strategy. Here we used the *cxcr3.2*^{hu604} mutant line to extend the functional study of the receptor in cell migration and bacterial infection. In this mutant line, a nonsense point mutation results in 96% truncation of the total *cxcr3.2* coding sequence. Using the mutant line, we first performed hindbrain ventricle injection at 28 hpf with *S. typhimurium* bacteria. Consistent with results of tail muscle injections in *cxcr3.2* morphants, deficiency of *cxcr3.2* in the mutant line led to reduction of macrophage recruitment at 3 hpi, supporting the contribution of Cxcr3.2 to bacterial-induced macrophage migration. However, bacterial-induced macrophage migration in *cxcr3.2* mutant embryos was only partially impaired at 3 hpi and almost recovered by 8 hpi. These effects indicate

that the early macrophage migration process is controlled by multiple factors, such as the formylpeptide receptors which directly sense the presence of bacteria (Le *et al*., 2007; Yang *et al*., 2008) and other chemokine receptors expressed in the macrophage population (Chapter 5). Interestingly, the Cxcr3.2-dependent migration function appeared to be specific for bacterial infection, due to the fact that chemically induced inflammation with $CuSO_4$ (d'Alençon *et al*., 2010) did not alter macrophage migration to damaged neuromasts in *cxcr3.2* mutant embryos (Supplementary Figure S2). Furthermore, *S. typhimurium* hindbrain injection attracted a higher number of macrophages than injection of a similar dose of *M. marinum* bacteria, and *cxcr3.2* mutation had a stronger effect on the *S. typhimurium*-induced migration than on the *M. marinum*-induced migration. These results suggest that chemokine ligands for Cxcr3.2 are secreted at a higher level upon *S. typhimurium* hindbrain infection than upon *M. marinum* hindbrain infection.

We found that Cxcr3.2 is also involved in *S. typhimurium*-induced macrophage migration at later stages of the infection process. The hindbrain infection data showed that the number of macrophages in the ventricle of mutant embryos was significantly less than that in wild type embryos at 24 hpi. Thus, despite that macrophage numbers were very similar at 8 hpi, the follow up recruitment of macrophages to the infection site was reduced in the *cxcr3.2* mutant. Moreover, the mean level of bacterial burden in the hindbrain at 24 hpi was significantly higher in the absence of *cxcr3.2*. In contrast, intravenous injection of *S. typhimurium* or *M. marinum* strains in one day old embryos did not result in significant differences in bacterial burden. The zebrafish embryonic macrophages are different from matured tissue macrophages in the adult in that they are not yet terminally differentiated and still present in the circulation (Herbomel *et al*., 1999). When intravenously injected bacteria come in direct contact with macrophages in the bloodstream, they can be engulfed without requirement of Cxcr3.2-guided macrophage migration. Taken together, our data suggest that Cxcr3.2 is involved in early and later stages of directional migration of macrophages towards tissue-localized bacteria, which has an important impact on infection control.

To analyse the function of Cxcr3.2 in *M. marinum* infection, different strains and mutants were employed in our study. One commonly used mutant is the RD1/ESX1 secretion system mutant strain (ΔRD1), which is known to cause reduced and delayed granuloma formation in zebrafish embryos compared to the wild type M strain (Volkman *et al*., 2004; Davis *et al*., 2009). In addition, we used FAM53, an isogenic mutant of the wild type E11 strain, which has a mutation at the *fadE33* gene encoding a probable acyl-CoA dehydrogenase that has a predicted function in lipid metabolism (Stoop *et al.,* 2011). The FAM53 mutant has a reduced ability to induce granuloma formation in zebrafish embryos, while replication in host cells is not affected (Stoop *et al*., 2011). First, we examined the growth of *M. marinum* strains in *cxcr3.2* mutant embryos through systemic infection to reveal the

role this receptor in inducing the formation of granuloma-like aggregates. Infection with wild type strain Mma20 showed that granuloma-like structures were formed in tissues at different locations in the *cxcr3.2* mutant. This finding suggests that *cxcr3.2*-deficient macrophages are still able to phagocytose circulating *M. marinum* in the bloodstream and in turn migrate into other tissues to initiate granuloma formation. We then monitored the progression of local hindbrain infection with *M. marinum* strains, in which guided immune cell migration is required for the entire process. Two mutant strains, ΔRD1 and FAM53, showed increased proliferation in the hindbrain of *cxcr3.2* mutant embryos by 5 dpi. Interestingly, we consistently observed more extracellular proliferation of wild type as well as mutant *M. marinum* strains in the hindbrain of *cxcr3.2* mutants. These findings support the essential role of Cxcr3.2 in recruiting macrophages able to restrict mycobacterial growth in the infected tissue. Based on the results of hindbrain infections with different mutant strains, the function of Cxcr3.2 during the early pathogenesis of *M. marinum* is summarized in a preliminary model (Fig. 9). We propose that the first infected macrophages in the hindbrain recruit new macrophages via bacterial virulence factors (RD1, FAM53) and that host inflammatory factors (including Cxcr3.2 ligands) further contribute to macrophage recruitment. Infection spreads to these newly recruited macrophages by phagocytosis of apoptotic macrophages as proposed by Davis and Ramakrishnan (2009). In the absence of important bacterial virulence factors, such as RD1 and FAM53, recruitment of healthy macrophages is reduced and consequently granuloma formation is delayed (Davis and Ramakrishnan, 2009; Stoop *et al*., 2011). Notably, in the absence of Cxcr3.2 the host-driven component of macrophage recruitment is affected, which leads to reduced recruitment of macrophages and delayed granuloma formation. Our data suggest that infections with ΔRD1 and FAM53 mutant strains lead to a combined reduction of both the bacterial-driven component and the host-driven component of macrophage recruitment, which results in extracellular growth of *M. marinum* in *cxcr3.2* mutants.

Human and murine CXCR3, together with their ligands CXCL9, CXCL10 and CXCL11, have been suggested to play important roles in *Mycobacterium tuberculosis* infection. During pulmonary tuberculosis of human patients, both T and B cells were found to express significantly higher levels of *CXCR3* than in healthy subjects (Pokkali and Das, 2009). Pulmonary *M. tuberculosis* infection of C57BL/6 wild type and *CXCR3-/-* mutant mice showed that early granuloma formation was regulated by neutrophils and depended on chemokine signaling through CXCR3 (Seiler *et al*., 2003). In contrast, the formation of caseating granulomas in C57BL/6 mice infected with *Mycobacterium avium* was not affected by *CXCR3* knockout (Aly *et al*., 2007). Remarkably, *CXCR3*-deficient BALB/c mice were more resistant to *M. tuberculosis*, compared with wild-type mice. This enhanced resistance manifested in the chronic but not the acute phase of infection and was associated with an increase in the number of $CD4^+$ T cells in the knockout

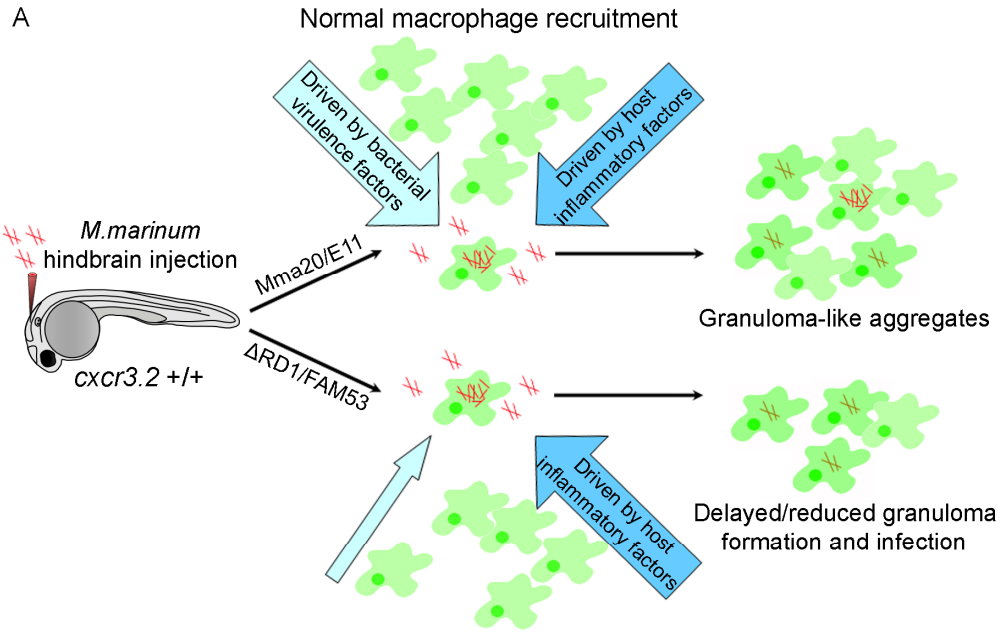
A
Normal macrophage recruitment
Driven by bacterial virulence factors
Driven by host inflammatory factors
M.marinum
hindbrain injection
Mma20/E11
ΔRD1/FAM53
cxcr3.2 +/+
Granuloma-like aggregates
Driven by host inflammatory factors
Delayed/reduced granuloma formation and infection
Bacterial driven macrophage recruitment reduced

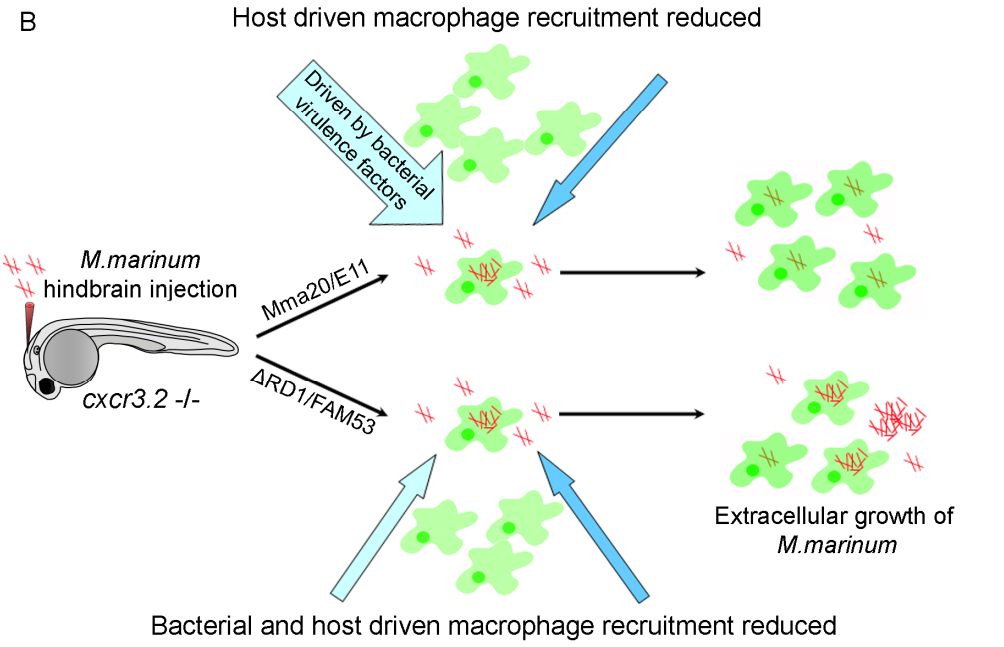
B
Host driven macrophage recruitment reduced
Driven by bacterial virulence factors
M.marinum
hindbrain injection
Mma20/E11
ΔRD1/FAM53
cxcr3.2 -/-
Extracellular growth of M.marinum
Bacterial and host driven macrophage recruitment reduced

Figure 9. Model of Cxcr3.2 signaling function during early *M. marinum* infection and granuloma formation. (A) Local infection of *M. marinum* in wild type embryos induces macrophage migration and phagocytosis at the infection site. Infected cells recruit new macrophages via bacterial virulence factors (RD1, Fam53) and host inflammatory factors (including Cxcr3.2 ligands). Infection spreads to these newly recruited macrophages by phagocytosis of apoptotic macrophages as proposed by Davis and Ramakrishnan (2009). Macrophage recruitment is reduced and consequently granuloma formation is delayed in the absence of bacterial virulence factors RD1 and Fam53 (Davis and Ramakrishnan, 2009; Stoop *et al.*, 2011). (B) In the absence of Cxcr3.2, the host-driven component of macrophage recruitment is affected. As a consequence, local hindbrain infection leads to reduced recruitment of macrophages and delayed granuloma formation. In *cxcr3.2* mutants infected with ΔRD1 and Fam53 mutant strains there is a combined reduction of both the bacterial-driven component and the host-driven component of macrophage recruitment, which leads to extracellular growth of *M. marinum*.

strain. These results suggest that CXCR3 plays an important role in modulating the cellular composition of tuberculous granulomas and can attenuate the host immune response to *M. tuberculosis* by adversely affecting T cell priming (Chakravarty *et al.*, 2007). The earliest stages of tuberculous granuloma formation are more accessible to observation in the *M. marinum*-zebrafish embryo model than in mammalian models of tuberculosis (Davis and Ramakrishnan, 2009; Ramakrishnan, 2012). Our analysis of *cxcr3.2* in this model revealed its importance for macrophage recruitment to *M. marinum* infection sites. Macrophage-specific functions for mammalian CXCR3 have also recently emerged (Zhou *et al*., 2010; Milićević *et al*., 2011; Cuenca *et al*., 2011). This makes a possible function of CXCR3 in responses of macrophages to *M. tuberculosis* especially worthy of investigation. In addition, adult zebrafish models of *M. marinum* infection, where adaptive immunity is present, will be useful for further analyzing CXCR3 family functions in tuberculosis, since adult zebrafish develop caseating granulomas with very similar structure to those in human patients.

The CXCL chemokine families of zebrafish and human have diverged more than the CXCR chemokine receptor families. Phylogeny relationships between zebrafish chemokines and human CXCR3 ligands are unclear, but a group of six zebrafish chemokines was identified that is relatively close to the human CXCL9/10/11 group (Chapter 3). We have shown that recombinant protein of one of these chemokines, Cxcl11, has chemoattractant activity on zebrafish embryonic macrophages (Chapter 3). In addition, *cxcl11* gene expression was found to be inducible by *M. marinum* infection. We therefore hypothesized that this chemokine might be responsible for Cxcr3.2-directed macrophage migration. Using the hindbrain injection site for *in vivo* chemotaxis studies revealed that Cxcl11-driven macrophage recruitment is significantly reduced in *cxcr3.2* mutants. While the receptor-ligand interaction needs to be confirmed by direct binding assays *in vitro*,

our *in vivo* analysis of Cxcl11 strongly supports its function as a putative ligand of Cxcr3.2. As five other CXC chemokines are also closely related to human CXCR3 ligands (Chapter 3), Cxcl11 may not be the only ligand for Cxcr3.2. Especially the gene annotated in NCBI as *cxcl11l* is a good candidate as this gene showed high induction at different stages of *S. typhimurium* and *M. marinum* infection. Furthermore, Cxcl11 might also interact with Cxcr3.1 or other receptors. In future work we aim to resolve all CXCL-CXCR ligand-receptor interactions in zebrafish using *in vitro* assays and the same *in vivo* strategy as for the Cxcl11-Cxcr3.2 interaction.

Acknowledgements

For providing the zebrafish knockout allele *cxcr3.2*^{hu6044} we thank the Hubrecht Laboratory and the Sanger Institute Zebrafish Mutation Resource (ZF-MODELS Integrated Project; contract number LSHG-CT-2003-503496; funded by the European Commission), also sponsored by the Welcome Trust; grant number WT 077047/Z/05/Z). We thank Marcel Schaaf for help with Imaris analysis. This work was supported by the Smart Mix Program of The Netherlands Ministry of Economic Affairs and the Ministry of Education, Culture and Science, and by the European Marie-Curie Initial Training Network FishForPharma (contract number PITN-GA-2011-289209).

References

d'Alencon, C. A.; Pena, O. A.; Wittmann, C.; Gallardo, V. E.; Jones, R. A.; Loosli, F.; Liebel, U.; Grabher, C.; Allende, M. L., A high-throughput chemically induced inflammation assay in zebrafish. *BMC Biol* **2010,** *8*, 151.

Aly, S.; Laskay, T.; Mages, J.; Malzan, A.; Lang, R.; Ehlers, S., Interferon-gamma-dependent mechanisms of mycobacteria-induced pulmonary immunopathology: the role of angiostasis and CXCR3-targeted chemokines for granuloma necrosis. *J Pathol* **2007,** *212* (3), 295-305.

Boldajipour, B.; Mahabaleshwar, H.; Kardash, E.; Reichman-Fried, M.; Blaser, H.; Minina, S.; Wilson, D.; Xu, Q.; Raz, E., Control of chemokine-guided cell migration by ligand sequestration. *Cell* **2008,** *132* (3), 463-73.

Chakravarty, S. D.; Xu, J.; Lu, B.; Gerard, C.; Flynn, J.; Chan, J., The chemokine receptor CXCR3 attenuates the control of chronic Mycobacterium tuberculosis infection in BALB/c mice. *J Immunol* **2007,** *178* (3), 1723-35.

Cuenca, A. G.; Wynn, J. L.; Kelly-Scumpia, K. M.; Scumpia, P. O.; Vila, L.; Delano, M. J.; Mathews, C. E.; Wallet, S. M.; Reeves, W. H.; Behrns, K. E.; Nacionales, D. C.; Efron, P. A.; Kunkel, S. L.; Moldawer, L. L., Critical role for CXC ligand 10/CXC receptor 3 signaling in the murine neonatal response to sepsis. *Infect Immun* **2011,** *79* (7), 2746-54.

Cui, C.; Benard, E. L.; Kanwal, Z.; Stockhammer, O. W.; van der Vaart, M.; Zakrzewska, A.; Spaink, H. P.; Meijer, A. H., Infectious disease modeling and innate immune function in zebrafish embryos. *Methods Cell Biol* **2011,** *105*, 273-308.

Dambly-Chaudiere, C.; Cubedo, N.; Ghysen, A., Control of cell migration in the development of the posterior lateral line: antagonistic interactions between the chemokine receptors CXCR4 and CXCR7/RDC1. *BMC Dev Biol* **2007,** *7*, 23.

Davis, J. M.; Clay, H.; Lewis, J. L.; Ghori, N.; Herbomel, P.; Ramakrishnan, L., Real-time visualization of mycobacterium-macrophage interactions leading to initiation of granuloma formation in zebrafish embryos. *Immunity* **2002,** *17* (6), 693-702.

Davis, J. M.; Ramakrishnan, L., The role of the granuloma in expansion and dissemination of early tuberculous infection. *Cell* **2009,** *136* (1), 37-49.

Davison, J. M.; Akitake, C. M.; Goll, M. G.; Rhee, J. M.; Gosse, N.; Baier, H.; Halpern, M. E.; Leach, S. D.; Parsons, M. J., Transactivation from Gal4-VP16 transgenic insertions for tissue-specific cell labeling and ablation in zebrafish. *Dev Biol* **2007,** *304* (2), 811-24.

Dumstrei, K.; Mennecke, R.; Raz, E., Signaling pathways controlling primordial germ cell migration in zebrafish. *J Cell Sci* **2004,** *117* (Pt 20), 4787-95.

Ellett, F.; Pase, L.; Hayman, J. W.; Andrianopoulos, A.; Lieschke, G. J., mpeg1 promoter transgenes direct macrophage-lineage expression in zebrafish. *Blood* **2011,** *117* (4), e49-56.

Fulton, A. M., The chemokine receptors CXCR4 and CXCR3 in cancer. *Curr Oncol Rep* **2009,** *11* (2), 125-31.

Groom, J. R.; Luster, A. D., CXCR3 in T cell function. *Exp Cell Res* **2011,** *317* (5), 620-31.

Haas, P.; Gilmour, D., Chemokine signaling mediates self-organizing tissue migration in the zebrafish lateral line. *Dev Cell* **2006,** *10* (5), 673-80.

Herbomel, P.; Thisse, B.; Thisse, C., Ontogeny and behaviour of early macrophages in the zebrafish embryo. *Development* **1999,** *126* (17), 3735-45.

Kanwal, Z., Regulatory mechanisms of innate immune signaling in zebrafish embryos. *Thesis, Leiden University* **2012**.

Kimmel, C. B.; Ballard, W. W.; Kimmel, S. R.; Ullmann, B.; Schilling, T. F., Stages of embryonic development of the zebrafish. *Dev Dyn* **1995,** *203* (3), 253-310.

Knaut, H.; Schier, A. F., Clearing the path for germ cells. *Cell* **2008,** *132* (3), 337-9.

Lacotte, S.; Brun, S.; Muller, S.; Dumortier, H., CXCR3, inflammation, and autoimmune diseases. *Ann N Y Acad Sci* **2009,** *1173*, 310-7.

Le, Y.; Wang, J. M.; Liu, X.; Kong, Y.; Hou, X.; Ruan, L.; Mou, H., Biologically active peptides interacting with the G protein-coupled formylpeptide receptor. *Protein Pept Lett* **2007,** *14* (9), 846-53.

Lee, E. C.; Yu, D.; Martinez de Velasco, J.; Tessarollo, L.; Swing, D. A.; Court, D. L.; Jenkins, N. A.; Copeland, N. G., A highly efficient Escherichia coli-based chromosome engineering system adapted for recombinogenic targeting and subcloning of BAC DNA. *Genomics* **2001,** *73* (1), 56-65.

Liu, L.; Callahan, M. K.; Huang, D.; Ransohoff, R. M., Chemokine receptor CXCR3: an unexpected enigma. *Curr Top Dev Biol* **2005,** *68*, 149-81.

Mahabaleshwar, H.; Boldajipour, B.; Raz, E., Killing the messenger: The role of CXCR7 in regulating primordial germ cell migration. *Cell Adh Migr* **2008,** *2* (2), 69-70.

Mathias, J. R.; Perrin, B. J.; Liu, T. X.; Kanki, J.; Look, A. T.; Huttenlocher, A., Resolution of inflammation by retrograde chemotaxis of neutrophils in transgenic zebrafish. *J Leukoc Biol* **2006,** *80* (6), 1281-8.

Milicevic, N. M.; Miljkovic, M. D.; Milicevic, Z.; Labudovic-Borovic, M.; Wang, X.; Laan, M.; Peterson, P.; Randall, T. D.; Westermann, J., Role of CCL19/21 and its possible signaling through CXCR3 in development of metallophilic macrophages in the mouse thymus. *Histochem Cell Biol* **2011,** *135* (6), 593-601.

Miyasaka, N.; Knaut, H.; Yoshihara, Y., Cxcl12/Cxcr4 chemokine signaling is required for placode assembly and sensory axon pathfinding in the zebrafish olfactory system. *Development* **2007,** *134* (13), 2459-68.

Moser, B., Chemokines: role in immune cell traffic. *Eur Cytokine Netw* **2003,** *14* (4), 204-10.

Moser, B.; Willimann, K., Chemokines: role in inflammation and immune surveillance. *Ann Rheum Dis* **2004,** *63 Suppl 2*, ii84-ii89.

Moser, B.; Wolf, M.; Walz, A.; Loetscher, P., Chemokines: multiple levels of leukocyte migration control. *Trends Immunol* **2004,** *25* (2), 75-84.

Muller, M.; Carter, S.; Hofer, M. J.; Campbell, I. L., Review: The chemokine receptor CXCR3 and its ligands CXCL9, CXCL10 and CXCL11 in neuroimmunity--a tale of conflict and conundrum. *Neuropathol Appl Neurobiol* **2010,** *36* (5), 368-87.

Nomiyama, H.; Hieshima, K.; Osada, N.; Kato-Unoki, Y.; Otsuka-Ono, K.; Takegawa, S.; Izawa, T.; Yoshizawa, A.; Kikuchi, Y.; Tanase, S.; Miura, R.; Kusuda, J.; Nakao, M.; Yoshie, O., Extensive expansion and diversification of the chemokine gene family in zebrafish: identification of a novel chemokine subfamily CX. *BMC Genomics* **2008,** *9*, 222.

Novoa, B.; Bowman, T. V.; Zon, L.; Figueras, A., LPS response and tolerance in the zebrafish (Danio rerio). *Fish Shellfish Immunol* **2009,** *26* (2), 326-31.

Oehlers, S. H.; Flores, M. V.; Hall, C. J.; O'Toole, R.; Swift, S.; Crosier, K. E.; Crosier, P. S., Expression of zebrafish cxcl8 (interleukin-8) and its receptors during development and in response to immune stimulation. *Dev Comp Immunol* **2010,** *34* (3), 352-9.

Pokkali, S.; Das, S. D., Augmented chemokine levels and chemokine receptor expression on immune cells during pulmonary tuberculosis. *Hum Immunol* **2009,** *70* (2), 110-5.

Ramakrishnan, L., Revisiting the role of the granuloma in tuberculosis. *Nat Rev Immunol* **2012,** *12* (5), 352-66.

Raz, E.; Mahabaleshwar, H., Chemokine signaling in embryonic cell migration: a fisheye view. *Development* **2009,** *136* (8), 1223-9.

Renshaw, S. A.; Loynes, C. A.; Trushell, D. M.; Elworthy, S.; Ingham, P. W.; Whyte, M. K., A transgenic zebrafish model of neutrophilic inflammation. *Blood* **2006,** *108* (13), 3976-8.

van der Sar, A. M.; Abdallah, A. M.; Sparrius, M.; Reinders, E.; Vandenbroucke-Grauls, C. M.; Bitter, W., *Mycobacterium marinum* strains can be divided into two distinct types based on genetic diversity and virulence. *Infect Immun* **2004,** *72* (11), 6306-12.

van der Sar, A. M.; Musters, R. J.; van Eeden, F. J.; Appelmelk, B. J.; Vandenbroucke-Grauls, C. M.; Bitter, W., Zebrafish embryos as a model host for the real time analysis of *Salmonella typhimurium* infections. *Cell Microbiol* **2003,** *5* (9), 601-11.

Seiler, P.; Aichele, P.; Bandermann, S.; Hauser, A. E.; Lu, B.; Gerard, N. P.; Gerard, C.; Ehlers, S.; Mollenkopf, H. J.; Kaufmann, S. H., Early granuloma formation after aerosol Mycobacterium tuberculosis infection is regulated by neutrophils via CXCR3-signaling chemokines. *Eur J Immunol* **2003,** *33* (10), 2676-86.

Stoop, E. J.; Schipper, T.; Huber, S. K.; Nezhinsky, A. E.; Verbeek, F. J.; Gurcha, S. S.; Besra, G. S.; Vandenbroucke-Grauls, C. M.; Bitter, W.; van der Sar, A. M., Zebrafish embryo screen for mycobacterial genes involved in the initiation of granuloma formation reveals a newly identified ESX-1 component. *Dis Model Mech* **2011,** *4* (4), 526-36.

Suster, M. L.; Abe, G.; Schouw, A.; Kawakami, K., Transposon-mediated BAC transgenesis in zebrafish. *Nat Protoc* **2011,** *6* (12), 1998-2021.

Ulrichs, T.; Kaufmann, S. H., New insights into the function of granulomas in human tuberculosis. *J Pathol* **2006,** *208* (2), 261-9.

Valentin, G.; Haas, P.; Gilmour, D., The chemokine SDF1a coordinates tissue migration through the spatially restricted activation of Cxcr7 and Cxcr4b. *Curr Biol* **2007,** *17* (12), 1026-31.

Volkman, H. E.; Clay, H.; Beery, D.; Chang, J. C.; Sherman, D. R.; Ramakrishnan, L., Tuberculous granuloma formation is enhanced by a mycobacterium virulence determinant. *PLoS Biol* **2004,** *2* (11), e367.

Yang, K. H.; Fang, H.; Ye, J. S.; Gong, J. Z.; Wang, J. T.; Xu, W. F., The main functions and structural modifications of tripeptide N-formyl-methionyl-leucyl-phenylalanine (fMLP) as a chemotactic factor. *Pharmazie* **2008,** *63* (11), 779-83.

Zakrzewska, A.; Cui, C.; Stockhammer, O. W.; Benard, E. L.; Spaink, H. P.; Meijer, A. H., Macrophage-specific gene functions in Spi1-directed innate immunity. *Blood* **2010,** *116* (3), e1-11.

Zhou, J.; Tang, P. C.; Qin, L.; Gayed, P. M.; Li, W.; Skokos, E. A.; Kyriakides, T. R.; Pober, J. S.; Tellides, G., CXCR3-dependent accumulation and activation of perivascular macrophages is necessary for homeostatic arterial remodeling to hemodynamic stresses. *J Exp Med* **2010,** *207* (9), 1951-66.

Supplementary data

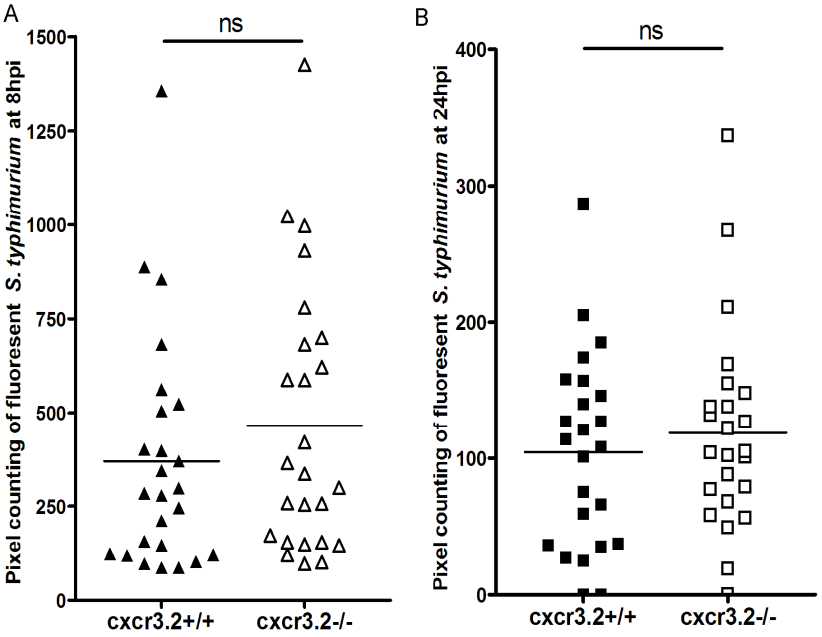

Figure S1. Quantification of systemic infections with *S. typhimurium* Ra in wild type and cx*cr3.2* mutant embryos. Intravenous infection with *S. typhimurium* Ra was performed by injection into the caudal blood island at 28 hpf. Quantification of infection levels by fluorescent pixel counting showed no significant difference between wild type and *cxcr3.2* mutant embryos at 8 hpi (A) and 24 hpi (B). Each data point represents an individual embryo and lines indicate the mean value. (ns, not significant, Student t-test).

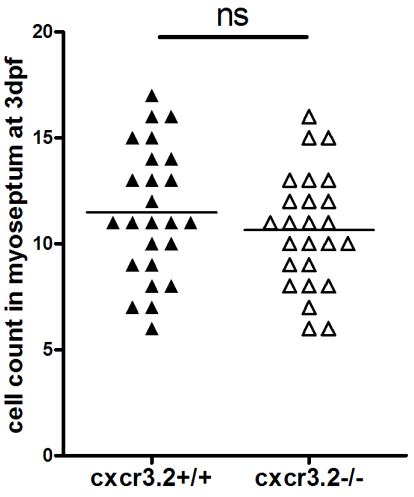

Figure S2. Normal macrophage migration in *cxcr3.2* mutant embryos in response to chemically-induced damage of lateral line neuromasts. Wild type and *cxcr3.2* mutant embryos were exposed at 3 dpf to 10 µM $CuSO_4$ for 2 hours as described (d'Alençon *et al.*, 2010). Treated embryos were fixed for combined L-plastin immuno and Mpx activity staining. Similar numbers of macrophages were recruited to $CuSO_4$-damaged neuromasts in wild type and *cxcr3.2* mutants. Each data point represents an individual embryo and lines indicate the mean value. (ns, not significant, Student t-test).